

Fractal and Chaotic Solutions of the Discrete Nonlinear Schrödinger Equation in Classical and Quantum Systems

H S DHILLON^{†1}, *F V KUSMARTSEV*^{†1†2} and *K E KÜRTE*^{†3}

^{†1} *Department of Physics, Loughborough University, LE11 3TU, UK*

^{†2} *Landau Institute, Moscow, Russia*

^{†3} *Institut für Experimentalphysik, Universität Wien, Austria*

Received May 8, 2000; Accepted August 30, 2000

Abstract

We discuss stationary solutions of the discrete nonlinear Schrödinger equation (DNSE) with a potential of the ϕ^4 type which is generically applicable to several quantum spin, electron and classical lattice systems. We show that there may arise chaotic spatial structures in the form of incommensurate or irregular quantum states. As a first (typical) example we consider a single electron which is strongly coupled with phonons on a 1D chain of atoms — the (Rashba)–Holstein polaron model. In the adiabatic approximation this system is conventionally described by the DNSE. Another relevant example is that of superconducting states in layered superconductors described by the same DNSE. Amongst many other applications the typical example for a classical lattice is a system of coupled nonlinear oscillators. We present the exact energy spectrum of this model in the strong coupling limit and the corresponding wave function. Using this as a starting point we go on to calculate the wave function for moderate coupling and find that the energy eigenvalue of these structures of the wave function is in exquisite agreement with the exact strong coupling result. This procedure allows us to obtain (numerically) exact solutions of the DNSE directly. When applied to our typical example we find that the wave function of an electron on a deformable lattice (and other quantum or classical discrete systems) may exhibit incommensurate and irregular structures. These states are analogous to the periodic, quasiperiodic and chaotic structures found in classical chaotic dynamics.

1 Introduction

Chaos is an important branch of nonlinear dynamics because chaotic behaviour seems to be universal [1]. It is present in mechanical oscillators, electrical circuits, lasers, nonlinear optical systems, chemical reactions, nerve cells, heated fluids and weather systems. Even more importantly, this chaotic behaviour shows qualitative and quantitative universal features which are independent of the details of the particular system and corresponds to a disappearance of periodic trajectories.

It is commonly believed that in quantum systems chaotic structures cannot arise. However, the question does arise if it would be possible to have in quantum systems a situation analogous to classical chaotic structures? In other words, if it would be possible for two slightly different boundary conditions or some physical parameters (for example, coupling constant) to correspond to two qualitatively different wave functions? Such dependence on physical conditions in quantum systems may be analogous to classical chaotic dynamics.

As classical chaotic motion is more obvious in time discrete systems which can be described, for example, by a discrete map ([1] and references therein), it is therefore only natural to study the quantum analogy of this phenomenon by considering the quantum effects in solids which are naturally discrete in space due to their atomic structure. Consequently, we study the atomic lattice taking into account a nonlinearity which arises due to electron-phonon interactions. This interaction gives rise to an apparent increase in the mass of the electron and causes the creation of some self-trapped (or polaronic) states. This phenomenon of the self-trapping of electrons and excitons in solids, originally predicted theoretically [2, 3, 4], has been observed and well studied in many materials (see, for example, review [5]). It arises, primarily, in low dimensional systems and in systems with a strong electron-phonon interaction. The (Rashba)–Holstein polaron model ([3, 4]) is described by a discrete nonlinear Schrödinger equation with a ϕ^4 type potential. Other systems which may be described by this generic equation include superconducting states in layered superconductors, film deposition in Surface Science and systems of coupled nonlinear oscillators.

2 The Hamiltonian and the DNSE

The classical and quantum systems mentioned above may be generally described with the use of the Hamiltonian

$$H = \sum_i |\psi_i - \psi_{i+1}|^2 - \sum_i \frac{c}{2} |\psi_i|^4 - E \sum_i |\psi_i|^2, \quad (1)$$

where ψ_i is (for the typical example) the wave function of the self-trapped particle on the i^{th} site, c is some (coupling) parameter and E is the energy eigenvalue. For coupled (nonlinear) oscillators the function ψ describes a lattice distortion. For quantum systems the wave function must, of course, satisfy the conventional normalization condition

$$\sum_i |\psi_i|^2 = 1 \quad (2)$$

which is effectively described when the eigenvalue E is used as a Lagrange multiplier. The parameter c may have both positive (for self-trapped quantum states) and negative (for nonlinear coupled oscillators) values depending on the system being studied.

The energetically favourable states of a system described by (1) correspond to the minima of (1). These states are described by $\hat{\nabla}H(\psi) \equiv 0$, where $\hat{\nabla}$ is the *differential operator* i.e. $\frac{\partial H}{\partial \psi_i}$. Differentiating (1) with respect to ψ_i gives the conventional discrete nonlinear Schrödinger equation (DNSE) of the form

$$-\psi_{i-1} + 2\psi_i - \psi_{i+1} - c|\psi_i|^2\psi_i = E\psi_i \quad (3)$$

which describes, amongst other things, the interaction of electrons and phonons [3, 4]. ψ_i is the wave function of the polaron (electron localized by interactions with phonons) so that $|\psi_i|^2$ is the charge density of the polaronic state, c is the electron-phonon coupling constant and E is the energy eigenvalue of this state. The normalization condition then gives the charge of the electron. The electron associated with a *small* polaron spends most of its time trapped on a single lattice site, that is, the majority of the charge is distributed on the localizing site and (in the continuum limit) the charge decays exponentially away from this lattice site.

For simplicity, only real solutions are discussed and so we make the substitution $|\psi_i|^2 = \psi_i^2$ in the DNSE. If we consider the discrete equation describing nonlinear harmonic oscillators we have

$$-x_{i-1} + 2x_i - x_{i+1} + cx_i^3 = ex_i \quad (4)$$

which differs from (3) in the sign of c . With the aid of the transformation

$$x_n = (-1)^n \psi_n, \quad (5)$$

$$e = 4 - E \quad (6)$$

we again get

$$-\psi_{i-1} + 2\psi_i - \psi_{i+1} - c\psi_i^3 = E\psi_i. \quad (7)$$

Thus, we find that all solutions and the classification of such solutions for the quantum problem associated with the DNSE with positive coupling constant ($c > 0$) are also the solutions (and corresponding classification) of the classical nonlinear lattices associated with negative coupling constant ($c < 0$).

Note that the behaviour of these solutions does not depend explicitly on the parameter c ; c can be rescaled or even scaled out. For example, for some scaling parameter β , ψ_i and c are related by the similarity transformation: $\psi_i \rightarrow \beta\psi_i$ and $c \rightarrow c/\beta^2$ [9]. The normalization condition is then given by $\sum_i \psi_i^2 = 1/\beta^2$.

3 Iterated maps

Conversion between Hamiltonian forms and mappings has long been known to be a powerful mathematical tool for the theoretical and numerical analysis of dynamical systems. Indeed, two-dimensional maps allow representation of a stationary configuration of a Hamiltonian of the form (1) by a trajectory of a dynamical system. Therefore, the mathematical situation is *identical* to that of temporal evolution, although the static problem has been formulated in terms of spatial arrangements. That is, we can apply adapted methods from the analysis of chaotic dynamical systems and explore the nature of possible solutions to the DNSE ie we can represent the DNSE (7) in the form of a $2D$ map ([6, 7, 8]).

Introducing the auxiliary variable $Z_{i+1} = \psi_{i+1} - \psi_i$ gives

$$Z_{i+1} = Z_i - E\psi_i - C\psi_i^3 \quad \text{and} \quad \psi_{i+1} = \psi_i + Z_{i+1} \quad (8)$$

which may be iterated after choosing arbitrary initial conditions. Numerical experiments investigating different trajectories of this $2D$ map have been performed for different values

of the parameters. We find that there are essentially only three types of phase portraits produced by iterating (8). They can be *regular* (periodic) where only a small number of points in the phase space are visited. There are also *irregular commensurate* (quasiperiodic) portraits in the form of closed loops. These loops consist of a number of points being visited in the phase space. As the commensurability decreases the points visited in the phase space become more and more dense and an elliptic orbit is mapped. Finally, we have *irregular incommensurate* portraits where the previous closed loops seem to be stochastically dispersed.

These phenomena, which are in agreement with previous work on the subject ([6, 7, 8]), indicate that in this system there are three qualitatively different types of orbits which depend on the values of the parameters: 1) periodic, 2) quasiperiodic and 3) chaotic. It is well known that the regular/commensurate solutions may be transformed into the quasiperiodic or chaotic type structures by a slight change of initial conditions or parameters.

Below we discuss an alternative method for solving (7) and present the spectrum of (7) in the large c limit. We then go on to apply a numerical method to our system of DNSEs and obtain results which we cannot reproduce with the above mapping procedure. These results are contrasted with those obtained using the iterated map technique and the spatial structure of the wave function is examined.

4 Exact solutions in the limit $c \rightarrow \infty$

The above DNSE (7) has exact solutions in the limit $c \rightarrow \infty$ for a N -site lattice, which have been published separately [10]. The associated energy eigenvalue of these exact solutions takes the form (for $c \gg 1$)

$$E = \frac{2m + 4l - c}{n}, \quad (9)$$

where the eigenvalue E intrinsically depends on both the structure of the wave function on the lattice — described by m, l, n — and on the parameter c . The structure of the wave function is such that it is localized, $\psi_i \neq 0$, on just n sites of the N -site lattice ($n \leq N$); on the remaining $N - n$ sites the wave function is zero, $\psi_i = 0$. Note that on each site where the (normalized) wave function is localized it takes a value of either $\psi_i = \pm 1/\sqrt{n}$ for all n sites — no other values are taken. These n localizing sites are separated into m spots — groups of neighbouring lattice sites on which the wave function is localized — and l kinks — change in the sign of the wave function on adjacent lattice sites — inside the spots. Between the spots the wave function is vanishing. Both m and l are less than or equal to n .

Eq. (9), obtained in the limit $c \rightarrow \infty$, has been compared with the exact and numerical solutions for various systems consisting of different numbers of sites. In all these cases for nearly all values of c (except small regions of critical values where the self-trapped solutions originate) there is perfect agreement with the derived formula (9). However, in contrast with this perfect agreement between eigenvalues, a decrease in the value of c leads to a noticeable deviation in the wave functions (eigenvectors) from those obtained in the limit $c \rightarrow \infty$.

The form of (9) suggests that as well as the ground state of the polaron ($E = 2 - c$) where the polaron is trapped on a single lattice site there also exist excited trapped states, for example $E = (2 - c)/2$, where the charge density of the polaron is distributed over 2 sites adjacent to one another. This is in contrast with previous work on this subject where the continuum approximation is made. We find that the continuum approximation is insufficient because it only describes the ground state of the system; there exist a whole host of excited states in a discrete system which simply do not exist in the continuum limit!

5 Exact numerical solutions for finite c

The first order corrections to the wave function (eigenvectors) obtained with the use of perturbation theory are of the order of \sqrt{n}/c ie $O(1/c)$. When the coupling constant c is not very large the wave functions of some states have interesting incommensurate and chaotic structures. Thus, from comparison with numerical results and with perturbation theory we conclude, that even though the spectrum of the DNSE for a system with a finite, arbitrary number, N , of sites is well described by equation (9) for $c \gg 1$, the shape of the appropriate wave function for smaller values of c may have only qualitative features of the wave function obtained in the limit $c \rightarrow \infty$. As c decreases the localization spots smear out. Since the spectrum, (9), is associated with a local localization pattern, it is universal and does not depend on the boundary conditions.

Although the structure of the wave function for $c \gg 1$ does not strongly agree with the structure of the wave function in the limit $c \rightarrow \infty$ we find that the wave function may be approximated reasonably well by an exponential function. This is only valid if the peaks in the wave function structure are separated sufficiently so that there is little or no interaction between the tails. For lattice sites sufficiently far away from the localized site we can assume that in (7) the value of the wave function is small so that the cubic nonlinear term is negligible, $\psi_i^3 \approx 0$. Then, in the continuum limit, we obtain a second order linear differential equation which may be expressed as

$$-\frac{\partial^2 \psi}{\partial x^2} = E\psi(x). \quad (10)$$

(10) has the asymptotic solution

$$\psi = A \exp\left(-\sqrt{-E}x\right), \quad (11)$$

where A is some parameter which from the normalisation condition goes as $A \sim (-E)^{1/4}$. (10) may only be used to describe the behaviour of the wave function sufficiently far away from the local maxima of the wave function because near the maxima the cubic nonlinear term cannot be neglected. Hence, away from the peak the behaviour of the wave function may be described as an exponential decay.

If a small perturbation in the asymptotic limit ($c \rightarrow \infty$) wave function $\Psi = (\psi_1, \psi_2, \dots, \psi_i, \dots, \psi_N)$ and energy eigenvalue E is considered then a correction to the wave function is revealed. This correction is found by starting with the asymptotic solution of the DNSE *but taking finite c* and successively applying the Newton–Raphson method until the corrections to the wave function become negligible and Ψ converges to some limit.

In matrix notation the N -dimensional Newton–Raphson method takes the form

$$\Psi(k+1) = \Psi(k) - \left[\hat{\nabla}^2 H(\Psi(k)) \right]^{-1} \hat{\nabla} H(\Psi(k)), \quad (12)$$

where $\Psi(k)$ is our wave function (vector) consisting of N components (N lattice sites) iterated k times — if $k = 0$ then it is simply the wave function in the asymptotic limit — and $\hat{\nabla}^2 H(\Psi(k))$ is (for 3 or more sites) a tridiagonal $N \times N$ matrix with diagonal elements $2 - E - 3c\psi_i^2(k)$, elements on either side of the diagonal = -1 and top-right and bottom-left elements = -1 for periodic boundary conditions (PBC).

This procedure is used until the correction to the wave function becomes negligible. This means that the wave function converges to some limit. This limit is an exact, numerical solution of the DNSE (7). Note that, as the corrections are of the form of a series with negative integral powers of c (ie first order correction $\sim 1/c$, second order correction $\sim 1/c^2$, etc), in the limit $c \rightarrow \infty$ the corrections are all zero and the asymptotic solutions are obtained.

The energy eigenvalue (for PBC) after each iteration step is given by

$$E(k) = \frac{-c \sum_i \psi_i^3(k)}{\sum_i \psi_i(k)} \quad (13)$$

and the value of $E(k)$ converges towards E for most values of $c \gg 1$ except for small regions of c where the localised states originate. Even in these sensitive regions the value of $E(k)$ is in fairly close agreement with E .

This process is, however, not always convergent. The wave vector may change structure when different eigenenergies have the same value or when the structure obtained from the asymptotic limit does not exist for a range of c . For example, for a 3 site system with PBC two of the eigenvalues are $-c/3$ and $(6 - c)/2$. Both of these eigenvalues have the same numerical value for $c = 18$ but they have very different structures of the wave function. It is possible for the initial wave vector structure corresponding to one energy eigenvalue to change during the iteration process to another structure which corresponds to a different energy eigenvalue. However, this new structure does also exist and is also a solution of the DNSE (7).

If during the numerical process there is a drastic change in E then this indicates that the wave function structure has changed and the iteration process will converge to some other limit.

Applying this method to the above DNSE for finite c taking the asymptotic solutions (which are exact in the limit $c \rightarrow \infty$) as the initial condition we may compare the results obtained with Newton’s method with the results obtained by the use of $2D$ iterated maps. For such a comparison, however, we have to introduce the new *phase space function* $\psi_{i+1} - \psi_i$ for the Newton procedure applied to the discrete system of equations and plot $\psi_{i+1} - \psi_i$ against ψ_i . This then allows us to compare the wave function structures obtained with the use of the Newton procedure and the trajectories of the $2D$ iterated maps discussed in Section 3. We find that as well as obtaining results from the two different methods which are consistent with each other we also obtain results from the Newton procedure which we could not get with the $2D$ maps. That is the pictures representing the phase space of our quantum system correspond to different periodic or chaotic spatial structures of the wave function.

6 Results

In the previous section we have reformulated our problem of the solution of a discrete nonlinear set of equations, (7), to a (discrete Newton–Raphson) iterative problem. This gives possible criteria for the classification of the solutions obtained. Following this iteration procedure we find that there exist different types of structures of the wave function; nonlinear localized solutions arise for $E < 0$. Our results indicate that there exist both regular and irregular types of structure of the wave vector for negative values of E . These structures may be akin to periodic, quasiperiodic and (deterministic) chaotic structures.

Of course for finite systems quasiperiodic and chaotic structures are not well defined because these are, strictly speaking, well defined only for systems of infinite size. However, we may still indicate analogous features, for example, with the aid of phase portraits adopted for finite size systems which are possibly equivalent to regular commensurate, irregular commensurate and irregular incommensurate structures of the wave function on the lattice.

6.1 Periodic trajectories

Fig. 1 shows the final (converged) behaviour of the wave function on the lattice (1a) and the corresponding phase portrait (1b) obtained by the Newton method described above for a 100 site lattice with Periodic Boundary Conditions (PBC). The initial structure consisted of a normalized wave function being localized on only 10 sites all equally spaced apart. Each of these localized sites is separated by 9 sites where the wave function is zero. The sign of the wave function alternated ie if it is positive at a particular site then the sign of the wave function 10 sites before or 10 sites after is negative. This gives rise to a period 20 structure on a 100 site lattice. The corresponding energy eigenvalue (given by (9)) is $E = (20 - c)/10$. Taking the coupling constant to be $c = 24$ and applying the above procedure to this initial structure of the normalized wave function we obtain the solution presented in Fig. 1a. This shows a periodic behaviour of the wave function through the lattice (as expected from the initial conditions). The corresponding phase portrait of the quantum state, Fig. 1b, indicates that this initial structure gives rise to a regular commensurate period 20 structure. The phase portrait consists of only 20 points as the wave function oscillates regularly.

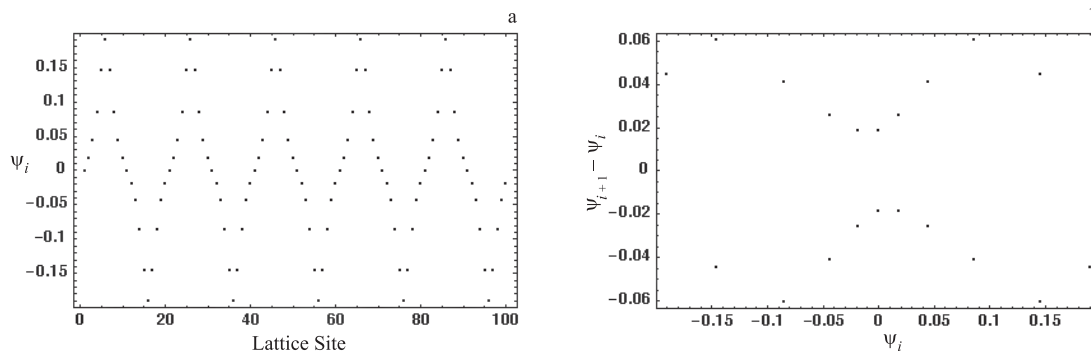


Figure 1.

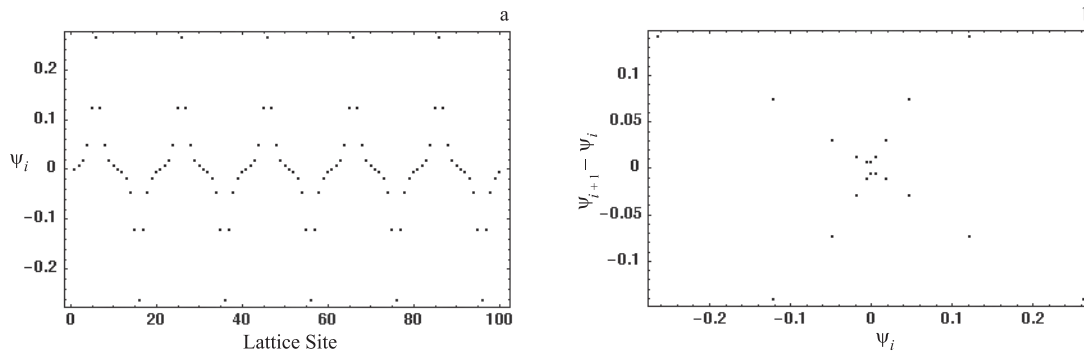


Figure 2.

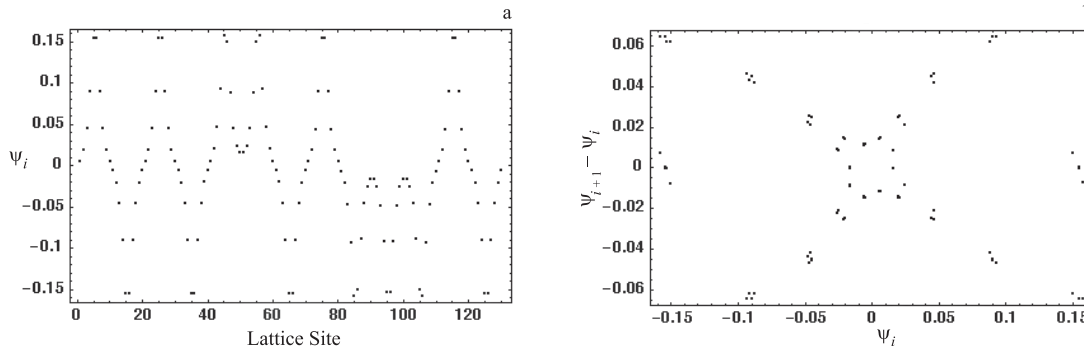


Figure 3.

Fig. 2 shows what happens as c is increased to $c = 30$. The width of each peak (or trough) decreases and the amplitude increases, that is, the wave function becomes more localized. In the limit $c \rightarrow \infty$ we will obtain our initial structure of the wave function being completely localized on the original 10 sites and zero everywhere else. Note that in this limit the corresponding phase space will consist of just 5 points: the origin $(\psi_i, \psi_{i+1} - \psi_i) = (0, 0)$, $(\psi_i, \psi_{i+1} - \psi_i) = (0, 1/\sqrt{n})$, $(\psi_i, \psi_{i+1} - \psi_i) = (0, -1/\sqrt{n})$, $(\psi_i, \psi_{i+1} - \psi_i) = (1/\sqrt{n}, -1/\sqrt{n})$ and $(\psi_i, \psi_{i+1} - \psi_i) = (-1/\sqrt{n}, 1/\sqrt{n})$.

6.2 Irregular trajectories

Fig. 3 shows the behaviour of the wave function on the lattice (3a) and the phase portrait (3b) for a 130 site lattice with PBC. The initial structure consisted of a normalized wave function being localized on 26 sites separated into 13 spots, each of which consisted of two localizing sites with the same sign of wave function. These spots were equally spaced apart and separated from each other by 8 sites where the wave function is zero. However, the sign of the wave function of different spots did not change regularly. The corresponding energy eigenvalue is $E = (26 - c)/26$. Taking the coupling constant to be $c = 40$ and applying the above procedure to this initial structure of the normalized wave function we obtain the solution presented in Fig. 3a. This shows an irregular oscillation of the wave function through the lattice although each of the peaks (and troughs) of the wave function are similar to one another. The corresponding phase portrait, Fig. 3b, maps out a double loop and near the origin is reminiscent of a hyperbolic point.

Again as c is increased the wave function becomes more localized and in the limit $c \rightarrow \infty$ we again obtain our initial structure of the wave function being completely localized on the original 26 sites and zero everywhere else. Note that in this limit the corresponding phase space will consist of 7 points: the five listed above and two more: $(\psi_i, \psi_{i+1} - \psi_i) = (1/\sqrt{n}, 0)$ and $(\psi_i, \psi_{i+1} - \psi_i) = (-1/\sqrt{n}, 0)$.

6.3 Random trajectories

Fig. 4 shows the behaviour of the wave function on a 208 site lattice for an arbitrary initial configuration. The energy eigenvalue given by (9) is $E = (86 - c)/63$. Taking $c = 260$ we obtain Fig. 4a where the behaviour of the wave function appears disordered. The wave function structure has split into three regions: top, middle and bottom. Fig. 4b shows the underlying pattern manifest in the wave function which consists of narrow peaks and troughs arranged in a pattern without any long-range order. The corresponding phase space, Fig. 4c, is in the form of a dispersed closed loop. This structure (which is reminiscent of chaos in classical systems) is due to the interaction of different localization spots. The appearance of a stochastic orbit indicates the effects of irregular incommensurability of the wave function on the lattice.

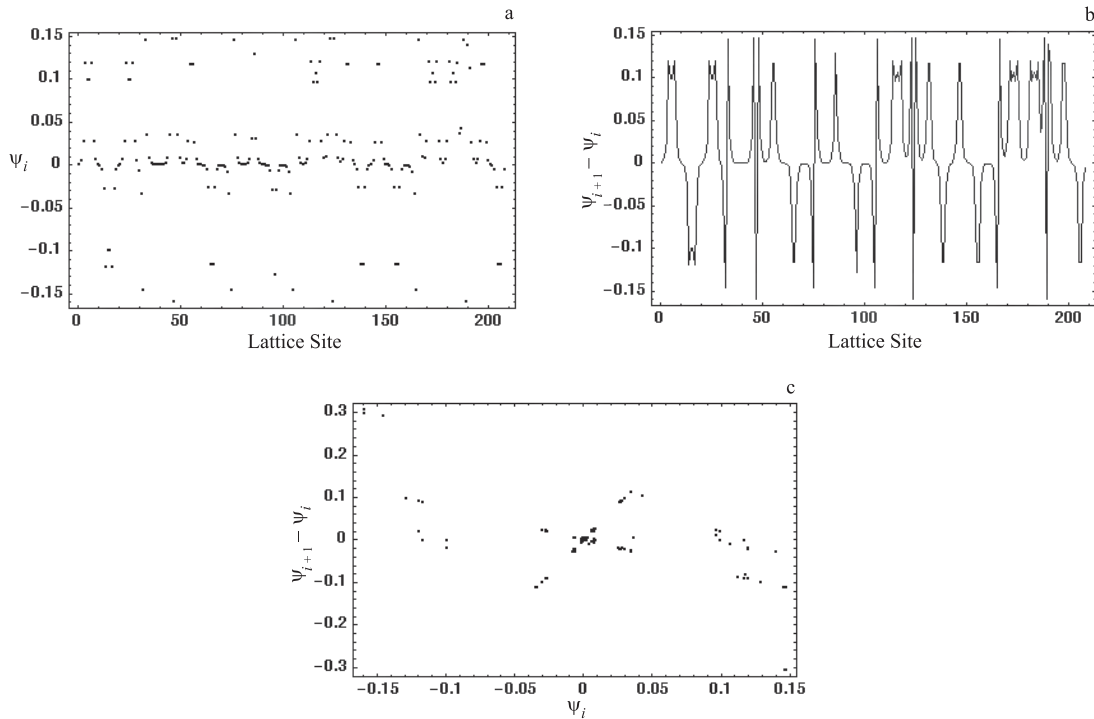


Figure 4.

Fig. 5 shows the behaviour of the wave function on a 1000 site lattice. The initial configuration was generated (pseudo-) randomly from the integers $-1, 0, 1$ and then normalized. The energy eigenvalue (from (9)) is $E = (1238 - c)/636$ and a value of $c = 4000$ gives the wave function structure shown in Fig. 5a. Again the wave function structure has split into top, middle and bottom. Fig. 5b shows the (dense) oscillations of the wave function and Fig. 5c is the phase portrait for this wave function. The points in this phase portrait

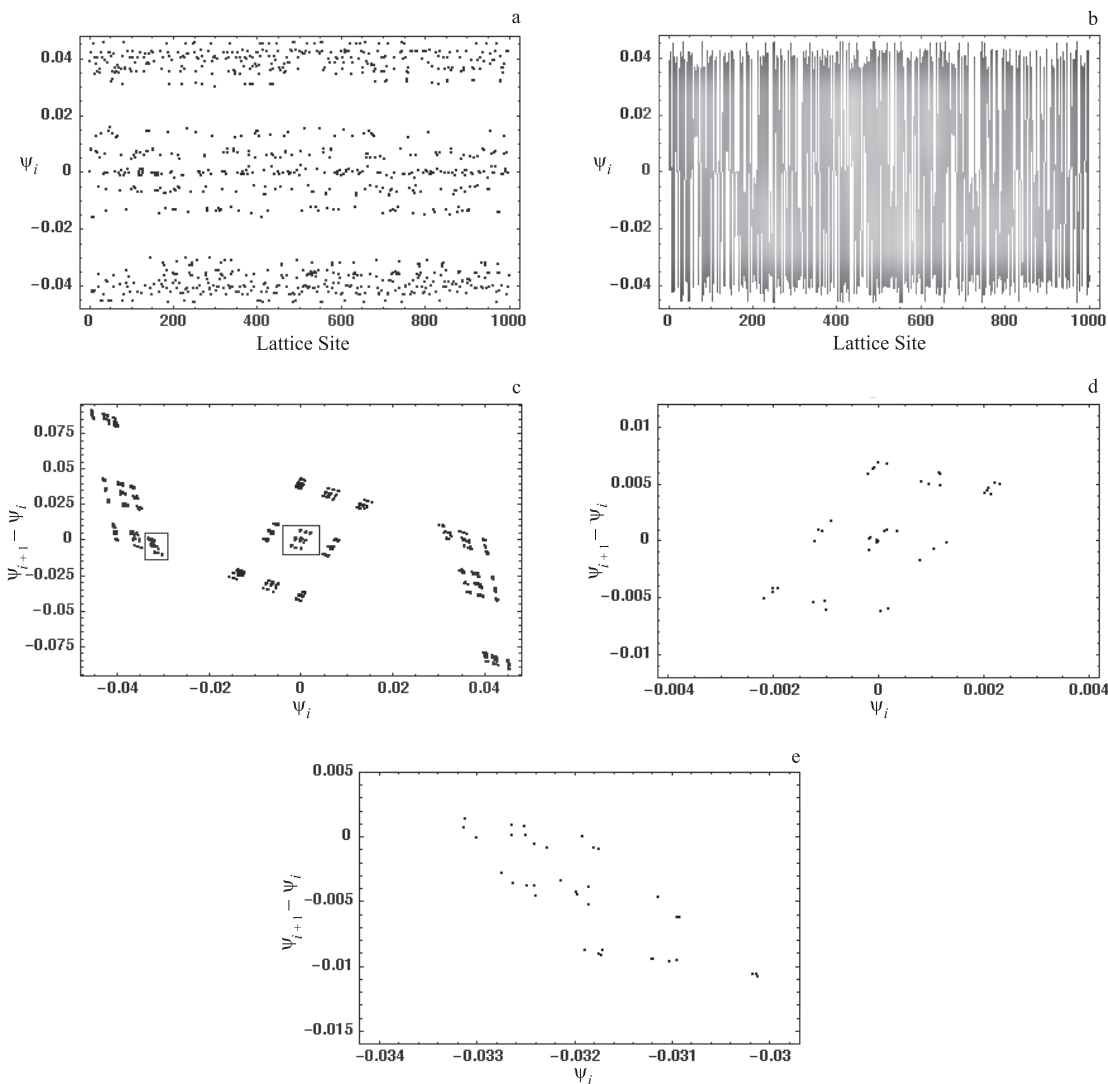


Figure 5.

don't seem to lie on an obvious closed loop or even a dispersed closed loop but rather a smeared curve. As this structure has no definite period it could be a possible candidate for a chaotic state of the system. The phase portrait is split into three parts: top-left, centre and bottom-right. Each of these three sections is further divided into sub-sections in which there appears a “nesting” of points. Something which is especially noticeable in the central part of this phase portrait is that each of the sub-sections are similar to the larger section in which they are contained.

For example, the boxed sub-section of nested points at the origin, which is magnified in Fig. 5d, is similar to the central section of Fig. 5c. The same trend can also be observed in other parts of the phase portrait, for example Fig. 5e is a magnification of the boxed region in the top-left segment of Fig. 5c. Both of these examples indicate a self-similarity in the structure of the wave function on a lattice. That is similar structures of the wave function exist on different length scales which suggests a fractal nature of the wave function on the lattice.

As the value of c is increased the different points visited in the phase space converge until only a maximum of nine points exist. These nine points which correspond to the wave function structure in the limit $c \rightarrow \infty$ are $(\psi_i, \psi_{i+1} - \psi_i) = (0, 0)$, $(\psi_i, \psi_{i+1} - \psi_i) = (0, 1/\sqrt{n})$, $(\psi_i, \psi_{i+1} - \psi_i) = (0, -1/\sqrt{n})$, $(\psi_i, \psi_{i+1} - \psi_i) = (1/\sqrt{n}, 0)$, $(\psi_i, \psi_{i+1} - \psi_i) = (1/\sqrt{n}, -1/\sqrt{n})$, $(\psi_i, \psi_{i+1} - \psi_i) = (1/\sqrt{n}, -2/\sqrt{n})$, $(\psi_i, \psi_{i+1} - \psi_i) = (-1/\sqrt{n}, 0)$, $(\psi_i, \psi_{i+1} - \psi_i) = (-1/\sqrt{n}, 1/\sqrt{n})$, $(\psi_i, \psi_{i+1} - \psi_i) = (-1/\sqrt{n}, 2/\sqrt{n})$.

7 Summary

Thus, we obtain that in the limit $c \rightarrow \infty$ there arises a degenerate set of solutions associated with different localization states of the polaronic wave function in the (Rashba)–Holstein model which consist of empty lattice sites (where the wave function is vanishing) and lattice sites where the wave function is localized. These localization patterns, which can be viewed as soliton type structures, have many different configurations which correspond to the same eigenvalue of the DNSE. However, when the value of c is not infinite this degeneracy is broken. Different localization spots within the pattern start to interfere with each other and modify the behaviour of the wave function. This leads to the existence of excited trapped states in this discrete system as well as the ground state. These excited trapped states may be experimentally observed by imaging the local density of states (LDOS). A finite amplitude of the LDOS fluctuations manifests correlations between fluctuations of local densities of individual wave functions at close energies. We go on to apply the Newton–Raphson method to this system of discrete nonlinear equations where, starting with the asymptotic solutions and iterating, $\Psi(k+1)$ is in general a better approximation to the solution of (7) than $\Psi(k)$ for finite c . This solution gives the structure of the wave function on the lattice and suggests the possible existence of fractal structures where the wave function structure at one scale is echoed at another scale.

The interaction between the solitons is essentially governed by the radius of the solitons and their separation and depends on the reciprocal of the modulus of an eigenvalue of the DNSE, $1/\sqrt{|E|}$, which governs the radius of the soliton peaks. If the radius of the soliton peaks is much smaller than the separation then we have regular, commensurate behaviour of the polaronic wave function on the lattice. In this case the interaction between the solitons is very weak. As the radius of the solitons increases ($1/\sqrt{|E|}$ increases) and the separation remains constant the interaction between the solitons increases and the behaviour of the wave function on the lattice becomes less regular. Finally, when the radius of the soliton peaks is about the same as the separation of the solitons we have strong interactions between the solitons. This results in strong incommensurability of the behaviour of the wave function on the lattice.

We find that the interference between the spots can give rise to three qualitatively different structures: periodic, quasiperiodic and chaotic. To indicate such structures in the quantum state the methods used in the studies of classical chaos were applied to the quantum system. A phase portrait was built up which consists of the amplitudes of the wave functions and of residues of these amplitudes associated with neighbouring sites. That is it is a projection of the Hilbert “phase space of our quantum system” in the plane, that is, the set $\{\psi_{i+1} - \psi_i, \psi_i\}$.

In the regular periodic and quasiperiodic solutions the wave function amplitudes replicate with some period equal to some integer number of lattice constants or creates aperiodic structures, respectively. However, there is also the appearance of structures analogous to the those arising in classical chaos which gives rise to self-similar structures of the wave function on the lattice at different length scales. The destruction of the periodic and quasiperiodic orbits, which has been ascribed to the creation of chaotic structure in the wave function, is also exhibited by the system. That is the creation of a structure which has no definite period has been found.

Acknowledgements

KEK gratefully acknowledges helpful assistance by R Valder at the computer center of the Heinrich-Heine University in Düsseldorf, by J Fertillet, J C Fiers and M Lams at the Université du Littoral in Dunkerque.

References

- [1] Hilborn R C, *Chaos and Nonlinear Dynamics*, Oxford University Press, New York, 1994.
- [2] Pekar S I, *Untersuchungen über die Electronentheorie des Kristallen*, Akedemie Verlag, Berlin, 1954.
- [3] Rashba E I, *Opt. Spectr.*, 1957, V.2, 78; V.2, 88.
- [4] Holstein T, *Ann. Phys.*, 1959, V.8, 343.
- [5] Rashba E I, in *Excitons*, Editors E I Rashba and M D Sturge, North-Holland, Amsterdam, 1982, 543.
- [6] Kusmartsev F V and Kürten K E, *Effects of Chaos in Quantum Lattice Systems*, in *Lecture Notes in Physics*, Editors J W Clark and M L Ristig, Springer-Verlag, New York – Heidelberg Berlin, 1997, V.284;
Kürten K E, in *Condensed Matter Theories*, Plenum, New York, 1999, V.13, V.14.
- [7] Bak P and Pokrovsky V L, *Phys. Rev. Lett.*, 1981, V.47, 958.
- [8] Aubry S, *J. de Physique*, 1983, V.44, 147.
- [9] Kusmartsev F V, Rashba E I, *Sov. Phys. JETP*, 1984, V.59, 668.
- [10] Kusmartsev F V and Dhillon H S, *Phys. Rev. B*, 1999, V.60, 6208.